HSPI The Open Access Publisher

IJPRA ISSN 2766-2748 INTERNATIONAL JOURNAL OF PHYSICS RESEARCH AND APPLICATIONS

Research Article

The Effect of Zero-range Pseudo-potential Approximation in the Elastic Scattering Channel Using A Mass-dependent M3Y-type Interaction

Raymond C Abenga*

Department of Pure and Applied Physics, Veritas University, Abuja, Nigeria

More Information

***Address for correspondence:** Raymond C Abenga, Department of Pure and Applied Physics, Veritas University, Abuja, Nigeria, Email: abengar@veritas.edu.ng

Submitted: June 20, 2025
Approved: June 25, 2025
Published: June 26, 2025

How to cite this article: Abenga RC. The Effect of Zero-range Pseudo-potential Approximation in the Elastic Scattering Channel Using A Mass-dependent M3Y-type Interaction. Int J Phys Res Appl. 2025; 8(6): 172-177. Available from: https://dx.doi.org/10.29328/journal.ijpra.1001126

Keywords: Angular distribution; Folding potential; Optical potential; Zero-range Pseudo-potential; M3Y-type interaction; S-matrix

Abstract

The angular distributions for the elastic scattering of a deuteron from ^{12}C were measured in the double model framework using a mass-dependent M3Y-type interaction. The optical potential of this study was derived using the double-folding formalism and subsequently employed in the optical model formalism to determine the reaction cross-sections of d + ^{12}C at different incident energies. The calculated differential cross-sections were analyzed and compared to experimental results. A good fit of the differential cross-section to the experimental data was achieved. The suitability of the fit affirms the present formulation as a suitable tool for the study of nuclear reactions and nuclear structure. The effect of including the imaginary potential and the s-matrix elements was also analyzed.

Introduction

The problem of nuclear scattering involves solving the Schrödinger equation for two interacting nuclei. This requires robust theoretical tools and models capable of reproducing fundamental nuclear matter properties such as binding energy, pressure, volume, susceptibility, and incompressibility [1-3]. Among these models, the Michigan 3-Yukawa (M3Y) interaction, derived from G-matrix elements of the harmonic oscillator potential, has been widely used and proven effective in studying nuclear structure and reactions.

In recent years, a variant of the M3Y interaction, known as the mass-dependent M3Y-type interaction, was developed using the Lowest-Order Constrained Variational (LOCV) method. This interaction incorporates mass dependence through parameters derived from nuclei with mass numbers 24, 40, and 90 [4]. Despite this mass dependence, the M3Y-type interaction was recommended for broader applications across different nuclei. However, its effect on reaction calculations remains insufficiently explored—a gap that forms the basis of the present study.

Determining the most appropriate form of nuclear potential to analyze interactions has been a longstanding focus in nuclear physics [5]. Both phenomenological and microscopic potentials have been developed and extensively used, particularly in elastic and non-elastic scattering channels [6]. Due to the presence of strong absorption effects in heavy-ion collisions, accurate modelling of the nuclear Optical Potential (OP) is essential. The real part of the OP is often derived using folding models, while the imaginary part, accounting for absorption, is typically modelled empirically [7,8].

The double-folding model combines realistic nucleon-nucleon (NN) interactions with nuclear density distributions to construct the real part of the OP [9]. This approach minimizes the ambiguities associated with phenomenological potentials [10]. Although folded potentials are inherently real, the imaginary component—representing absorption—can be included phenomenologically or through density-dependent corrections.

This study applies the double-folding model using the mass-dependent M3Y-type interaction to analyze the elastic scattering of a deuteron from ^{12}C. The primary goal is to assess the impact of the zero-range pseudo-potential and the mass-

dependent interactions on scattering predictions and compare the resulting cross-sections with experimental data. Both the real and imaginary parts of the optical potential are evaluated using folding techniques, and the fits to experimental angular distributions are examined to determine the model's accuracy.

B3Y-Fetal Effective Interaction

This study adopts the isoscalar component of the central potential from the mass-dependent M3Y-type interaction, as outlined in prior work [4]. The direct and exchange components of this interaction are given by [11,12]:

$$V_{00}^{D}(r) = 7419.23\frac{e^{-4r}}{4r} - 1823.98\frac{e^{-2.5r}}{2.5s} \quad (1)$$

Similarly, the exchange term is determined as:

$$V_{00}^{Ex}(r) = 4745.02\frac{e^{-4s}}{4s} - 1984.144\frac{e^{-2.5r}}{2.5r} - 7.8474\frac{e^{-0.7072r}}{0.7072r} \quad (2)$$

where $v_{00}^{D}(s)$, and $v_{00}^{Ex}(s)$ are the direct and exchange parts of the isoscalar central B3Y-Fetal interaction.

The bare nucleon-nucleon (NN) interactions alone are inadequate in reproducing the saturation properties of nuclear matter. To correct this, a density-dependent factor $f(\rho)$ is introduced, ensuring that the interaction achieves nuclear matter saturation [13]. This density dependence is expressed as [14,15]:

$$V_{00}^{D(Ex)}(\rho,r) = f(\rho)V_{00}^{D(Ex)}(r) \quad (3)$$

Concerning the density dependence, an exponential form of the density-dependent term was adopted [16,17]:

$$f(\rho) = C\left(1+\alpha\ \exp(-\beta\rho)\right) \quad (4)$$

Here, C and β are constants determined to reproduce the correct binding energy and saturation density of symmetric nuclear matter. These constants are obtained from prior parameterizations [18].

The exchange term is analyzed using the resonating-group method in a single-channel approximation [19]. It includes both single-nucleon and core exchange effects, significant primarily when projectile and target nuclei have similar mass numbers. To localize the otherwise nonlocal exchange term, a zero-range pseudo-potential is added, yielding [13]:

$$V_{pt} \rightarrow V_{pt}\left(1-P_{pt}\right) \quad (5)$$

Where V_{pt} are the direct and exchange parts of the effective interaction, P_{pt} is the operator that exchanges all the coordinates of the two nucleons by making the exchange part of the effective interaction local. By the zero-range pseudo-potential of equation (5), the interaction V_{pt} is transformed in the form [20,21],

$$V_{pt}\left(1-P_{EX}\right) \rightarrow V_{pt}(r) + \hat{J}(E)\delta(r) \quad (6)$$

where the function $\hat{J}(E) = J_{00}g(E)$ represents the zero-range pseudo-potential that incorporates the exchange component of the M3Y-type interaction [22-28]. The term, $V_{pt}(r)$, is the direct part of the isoscalar interaction defined by Equation (1) but now expressed as the projectile-target interaction. The term g(E) represents the energy scaling factor. The magnitude of the exchange amplitude J_{00} was evaluated to be about −361MeV [11,18]. The energy scaling factor was approximated to be $\left[1-0.005\left(\frac{E}{A}\right)\right]$.

The double-folding model

To construct the nuclear optical potential, the double-folding model was used. The double-folding model convolves the effective NN interaction with the nuclear density distributions of the projectile and target [19]:

$$V_F(r) = \iint \rho_p(\mathbf{r}_p)\rho_t(\mathbf{r}_t)V_{pt}(\mathbf{r}_{tp})d\mathbf{r}_p d\mathbf{r}_t \quad (7)$$

Where ρ_p and ρ_t are the density distributions of the projectile and target nuclei, and $r_{tp} = r_t - r_p$. The nuclear densities are modelled using a two-parameter Fermi (2pF) distribution [29-31]:

$$\rho_{n(p)}(r) = \rho_{0n(p)}\left[1+\exp\left(\frac{r-R_{p(n)}}{a_{p(n)}}\right)\right]^{-1} \quad (8)$$

Here, ρ_o is the central density, and $a_{p(n)}$ are the half-density radius and the diffuseness parameter, respectively. These parameters are obtained from empirical fits to charge distributions [26].

The double-folded potential naturally represents the real part of the optical potential. To account for the imaginary part—which captures absorption into non-elastic channels—a similar folding approach is applied but with a different renormalization factor [27]:

$$U(r) = \left(N_r + iN_i\right)V_F(r) + V_{Coul}(r) \quad (10)$$

Where $N_{r(i)}$ are the real and imaginary renormalization factors for the real and imaginary parts of the optical potential, and $V_{Coul}(r)$ is the Coulomb potential. These renormalization constants are adjusted to achieve optimal agreement with experimental data.

Results

Folding Model Potential of the Elastic Scattering of $d + {}^{12}C$

The double-folding model was employed to calculate the real and imaginary parts of the optical potential for the elastic scattering of a deuteron from ^{12}C at incident laboratory energies of 28, 110, 120, and 170 MeV. Using these potentials, the reaction and total cross-sections were computed and compared with those obtained using both phenomenological and microscopic potentials. The results are presented in Table 1.

The results indicate good agreement between the calculated reaction cross-sections and existing literature [28-

Table 1: Best-fit parameters and cross-sections for elastic scattering of d + ^{12}C.

Target	E_{lab}(MeV)	N_r	N_i	σ_r (mb)	σ_{tot} (mb)
^{12}C	28	1.00	0.80	977.95	1671.11
	110	1.60	1.00	752.84	1416.83
	120	1.70	1.00	730.08	1401.19
	170	1.45	0.90	578.19	1119.98

33], confirming the reliability of the double-folding approach. The optical potentials generated in this study exhibited typical Woods-Saxon shapes, and the values of the renormalization factors $N_{r(i)}$ reflect strong absorption effects at higher energies. The plots of the radial dependence of the strength of the folded potentials are shown in Figures 1-4. The potentials were attractive and short-ranged over small nuclear distances.

Analysis of the Differential Cross Section of the Elastic Scattering of d + ^{12}C

The plots of the angular distributions of the elastic scattering for each incident energy are shown in Figures 5-8.

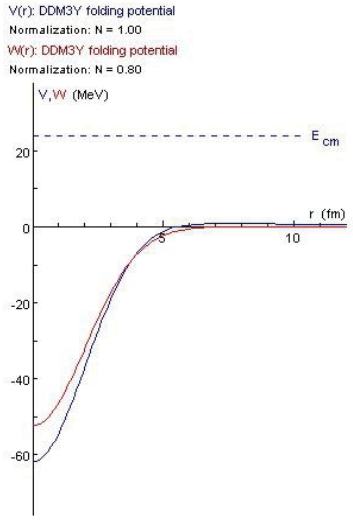

Figure 1: The depth of the real and imaginary folded potential of d + ^{12}C elastic scattering at E_{lab} = 28 MeV.

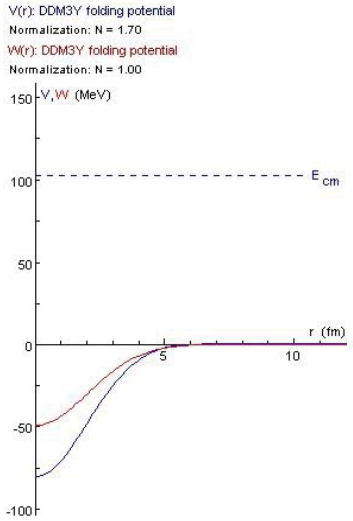

Figure 2: The depth of the real and imaginary folded potential of d + ^{12}C elastic scattering at E_{lab} = 120 MeV.

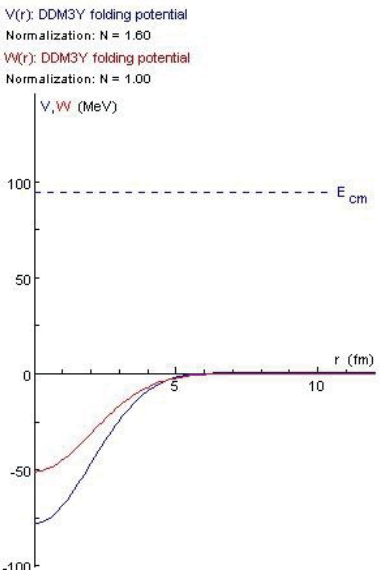

Figure 3: The depth of the real and imaginary folded potential of d + ^{12}C elastic scattering at E_{lab} = 110 MeV.

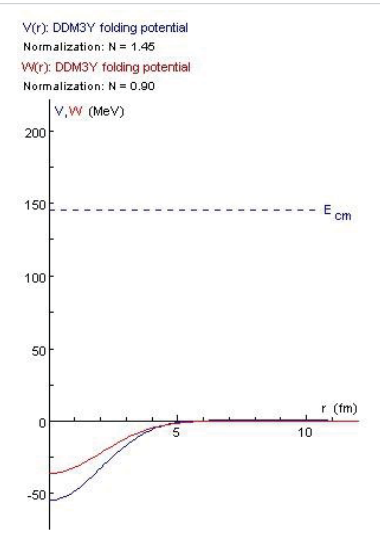

Figure 4: The depth of the real and imaginary folded potential of d + ^{12}C elastic scattering at E_{lab} = 170 MeV.

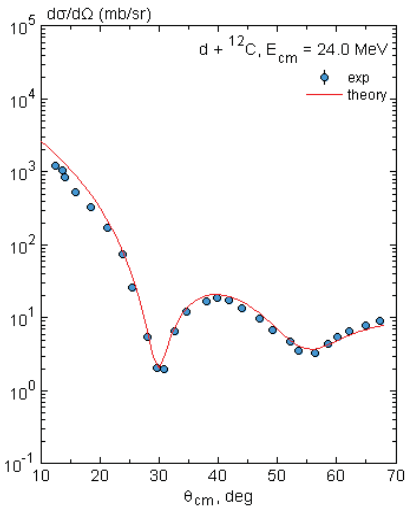

Figure 5: Angular distribution of d + ^{12}C elastic scattering at E_{lab} = 28 MeV.

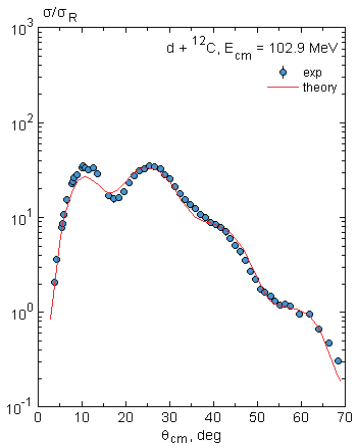

Figure 6: Angular distribution of d + ^{12}C elastic scattering at E_{lab} = 120 MeV.

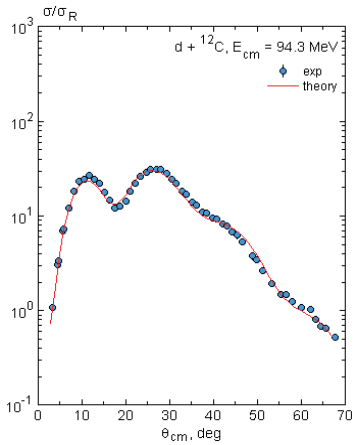

Figure 7: Angular distribution of d + ^{12}C elastic scattering at E_{lab} = 110 MeV.

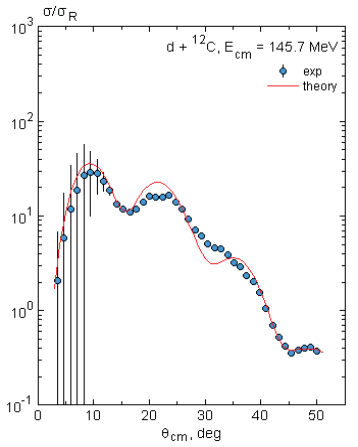

Figure 8: Angular distribution of d + ^{12}C elastic scattering at E_{lab} = 170 MeV.

The theoretical differential cross-sections match well with experimental data across all angles. The large X^2 value at 170 MeV suggests statistical anomalies or increased sensitivity in the data fitting (Table 2).

The experimental data points were reproduced quite accurately at all energies and angular regions. However, in the data of 170 MeV, a maximum and minimum were observed between $15^0 \leq \theta_{cm} \leq 25^0$ and $25^0 \leq \theta_{cm} \leq 35^0$. In general, a good fit of the theoretical calculations to experimental data was obtained, and a pronounced improvement in the fit of the differential cross-sections using the present formulation was achieved as compared to those obtained using microscopic and phenomenological potentials [28,30,31]. The plots of the modulus of the S-matrix elements are also shown in Figures 9-12 as a function of total orbital angular momentum ***L*** for the different incident energies. These plots reveal regions where $|S_L| < 1$, indicating strong absorption and the presence of other nonelastic processes. At 28 MeV, strong absorption is observed at small impact parameters in the angular momentum range $L \approx 0$ - 10. As energy increases, the contributing angular momentum values shift to higher L, indicating deeper penetration and more peripheral scattering contributions. This transition is consistent with the behaviour of the nuclear optical potential at different energies.

Table 2: Derived geometrical parameters of the optical potentials of d + ^{12}C.

Target	E_{lab} MeV	V_r MeV	r_v (fm)	a_v (fm)	W_i MeV	r_w (fm)	a_w (fm)	x^2
^{12}C	28	61.00	0.91	0.57	50.00	0.75	1.49	10.66
	110	75.00	0.67	0.90	27.36	0.91	0.63	2.09
	120	76.00	0.67	0.98	25.77	0.96	0.57	4.43
	170	52.00	0.78	0.86	25.00	0.98	0.61	3876440.21

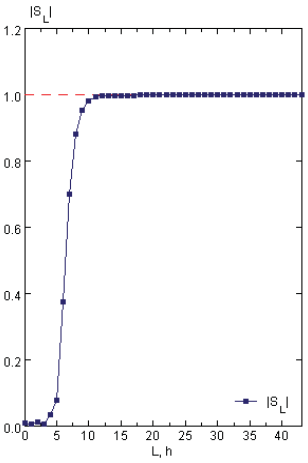

Figure 9: Modulus of the elastic S-matrix as a function of total orbital angular momentum of d + ^{12}C at E_{lab} = 28 MeV.

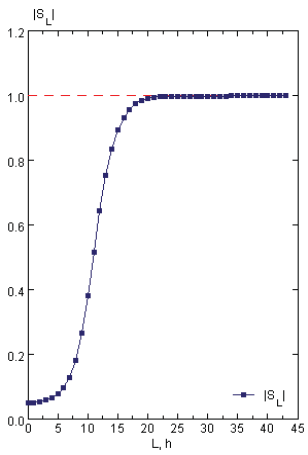

Figure 10: Modulus of the elastic S-matrix as a function of total orbital angular momentum of d + ^{12}C at E_{lab} = 110 MeV.

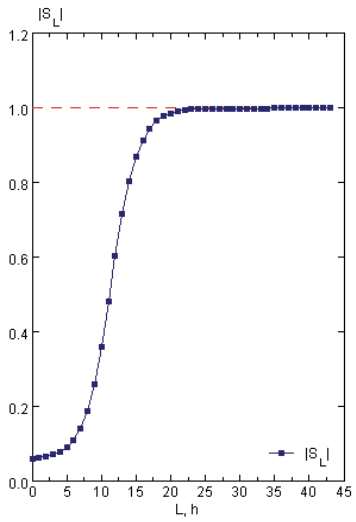

Figure 11: Modulus of the elastic S-matrix as a function of total orbital angular momentum of d + ^{12}C at E_{lab} = 120 MeV.

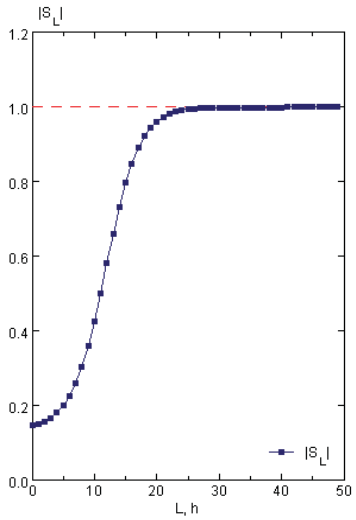

Figure 12: Modulus of the elastic S-matrix as a function of total orbital angular momentum of d + ^{12}C at E_{lab} = 170 MeV.

Conclusion

This study has employed the double-folding model in conjunction with the mass-dependent M3Y-type interaction to investigate the elastic scattering of [insert specific nuclei] over a range of incident laboratory energies (28–170 MeV). The analysis incorporated both the real and imaginary components of the optical potential derived through folding procedures, accounting for strong absorption effects observed in heavy-ion collisions. The calculated reaction and total cross-sections, as well as differential angular distributions, show excellent agreement with experimental data, validating the effectiveness of the M3Y-type interaction in modelling nuclear scattering phenomena. The renormalization factors obtained for the optical potentials reflect the expected energy dependence, and the folded potentials exhibit Woods-Saxon-like shapes consistent with known nuclear interaction behaviours.

Furthermore, the analysis of the elastic S-matrix elements revealed that nuclear contributions are most significant at small impact parameters and are gradually suppressed with increasing angular momentum, leaving the Coulomb interaction dominant at large distances. This confirms the realistic absorption effects modelled by the imaginary component of the potential. Overall, the results highlight the success of the mass-dependent M3Y-type interaction and the double-folding model in accurately reproducing scattering observables. It also demonstrated that the M3Y-type interaction is a robust tool for studying both elastic and potentially non-elastic nuclear reactions. These findings encourage future applications of this approach in other nuclear systems and energy regimes.

References

1. Abenga RC, Ibrahim YY, Adamu ID, Ibrahim L. Strong absorption and the double-folding potential using B3Y-fetal interaction. Caliphate J Sci Technol. 2024;6(3):323–32. Available from: http://dx.doi.org/10.4314/cajost.v6i3.9
2. Abenga RC, Ibrahim YY, Adamu ID. The folding potential of elastically scattered d + 24Mg employing B3Y-fetal interaction within the double folding model framework. UMYU Sci. 2024;3(3):239–50. Available from: https://orcid.org/0000-0001-7040-9395
3. Loan DT, Tan NH, Khoa DT, Margueron J. Equation of state of neutron star matter, and the nuclear symmetry energy. Phys Rev C. 2011;83(065809):1–16. Available from: https://journals.aps.org/prc/abstract/10.1103/PhysRevC.83.065809
4. Fiase JO, Devan KRS, Hosaka A. Mass dependence of M3Y-type interactions and the effects of tensor correlations. Phys Rev C - Nucl Phys. 2002;66(1):1–13. Available from: https://journals.aps.org/prc/abstract/10.1103/PhysRevC.66.014004
5. Kurkcuoglu ME, Aytekin H, Boztosun I. An investigation of the 16O + 16O elastic scattering by using the alpha-alpha alpha-double folding potential in optical model formalism. Mod Phys Lett A. 2006;21(29):2217–32. Available from: http://dx.doi.org/10.1142/S0217732306020512
6. El-Hammamy MN, Ibraheem AA, Branch A, Farid ME Azab, Elshamy EF. Comprehensive examination of the elastic scattering angular distributions of 10C + 4He, 27Al, 58Ni, and 208Pb using various potentials. Rev Mex Fisica. 2023;69:1–13. Available from: https://doi.org/10.31349/RevMexFis.69.031201
7. Amer HA, Amar A, Hamada S, Bondouk II, El-Hussiny FA. Optical and double-folding model analysis for alpha particles elastically scattered from 9Be and B nuclei at different energies. World Acad Sci Eng Technol Open Sci Index 110, Int J Chem Mol Eng. 2016;10(2):161–6. Available from: https://www.researchgate.net/publication/301650064_Optical_and_Double_Folding_Model_Analysis_for_Alpha_Particles_Elastically_Scattered_from_9Be_and_11B_Nuclei_at_Different_Energies
8. Kurkcuoglu ME, Aytekin H, Boztosun I. Optical model analysis of the 16O + 16O nuclear scattering reaction around E LAB = 5 MeV/nucleon. G U J Sci. 2006;19(2):105–12. Available from: https://dergipark.org.tr/tr/download/article-file/83089
9. Farid ME Azab, Mahmoud ZMM, Hassan GS. Analysis of heavy ions elastic scattering using the double folding cluster model. Nucl Phys A. 2001;691:671–90. Available from: https://doi.org/10.1016/S0375-9474(01)00587-5
10. Farid ME Azab. Heavy ion double folding cluster optical potentials. Phys Rev C. 2002;65(June):11–3. Available from: https://journals.aps.org/prc/abstract/10.1103/PhysRevC.65.067303
11. Abenga RC, Fiase JO, Ibeh GJ. Optical model analysis of α + Ca at E = 104 and 141.7 MeV using a mass-dependent M3Y-type effective interaction.

Niger Ann Pure Appl Sci. 2020;3(2):252–60. Available from: https://doi.org/10.46912/napas.144

12. Abenga RC, Fiase JO. Elastic scattering of 12C+12C and 16 O+16 O using an effective mass dependent M3Y-type interaction. Int J Innov Res Adv Stud. 2019;6(2):57–61. Available from: https://www.researchgate.net/publication/289393621_Elastic_scattering_of_12C_12C_16O_12C_16O_16O_and_nucleus-nucleus_potential_with_repulsive_core
13. Zang GL, Zang HQ, Liu ZH, Zang CL, Lin CJ, Yang F, et al. Double-folding model calculation applied to the real part of interaction potential. High Energy Phys Nucl Phys. 2007;13(7):634–41. Available from: http://dx.doi.org/10.3321/j.issn:0254-3052.2007.07.007
14. Moharram SA, El-Shal AO. Spin polarized cold and hot dense neutron matter. Turk J Phys. 2002;26:167–77. Available from: https://journals.tubitak.gov.tr/cgi/viewcontent.cgi?article=1884&context=physics
15. Hamada S, Bondok I, Abdelmoatmed M. Double folding potential of different interaction models for 16O + ^{12}C elastic scattering. Brazilian J Phys [Internet]. 2016;1–6. Available from: http://dx.doi.org/10.1007/s13538-016-0450-3
16. Khoa DT, Von Oertzen W. A nuclear matter study using the density-dependent M3Y interaction. Phys Lett B. 1993;304(12):8–16. Available from: https://doi.org/10.1016/0370-2693(93)91391-Y
17. Khoa DT, Von Oertzen W, Ogloblin AA. Study of the equation of state for asymmetric nuclear matter and interaction potential between neutron-rich nuclei using the density-dependent M3Y interaction. Nucl Phys A. 1996;602:98–132. Available from: https://doi.org/10.1016/0375-9474(96)00091-7
18. Abenga RC, Yahaya YI, Adamu ID. Double-folding potential of deuteron elastic scattering on target nuclei in the mass range of 50 ≤ A ≤ 208 using a mass-dependent effective interaction. Bayero J Phys Math Sci. 2021;01(13):1–14. Available from: https://www.scirp.org/reference/referencespapers?referenceid=3458338
19. Satchler GR, Love WG. Folding model potentials from realistic interactions for heavy-ion scattering. Phys Reports (Review Sect Phys Lett). 1979;55(3):183–254. Available from: https://www.scirp.org/reference/referencespapers?referenceid=3458333
20. Brandan ME, Satchler GR. The interaction between light heavy-ions and what it tells us. Phys Rep. 1997;285:143–243. Available from: https://doi.org/10.1016/S0370-1573(96)00048-8
21. Love WG, Owen LW. Exchange effects from realistic interactions in the reformulated optical model. Nucl Phys A. 1975;239:74–82. Available from: https://doi.org/10.1016/0375-9474(75)91133-1
22. Modarres M, Rahmat M. The LOCV averaged two-nucleon interactions versus the density-dependent M3Y potential for the heavy-ion collisions. Nucl Phys A [Internet]. 2015;934:148–66. Available from: http://dx.doi.org/10.1016/j.nuclphysa.2014.11.006
23. Satchler GR. A simple, effective interaction for peripheral heavy-ion collisions at intermediate energies. Nucl Phys A. 1994;579:241–55. Available from: https://doi.org/10.1016/0375-9474(94)90804-4
24. El-Attar AL, Farid ME Azab, El-Aref MG. Optical model analyses of deuteron inelastic scattering. In: 9th International Conference for Nuclear Sciences and Applications, Sharm Al Sheikh (Egypt). Egypt, 2008. p. 1239. Available from: https://inis.iaea.org/records/yq5wa-rxe20
25. De Vries H, De Jager CW, De Vries C. Nuclear charge-density-distribution parameters from elastic electron scattering. At Data Nucl Data Tables. 1987;36(3):495–536. Available from: " https://doi.org/10.1016/0092-640X(87)90013-1
26. Olorunfunmi SD, Olatinwo AS. Analysis of elastic scattering cross sections of 16O on 27Al and 154Sm using the semi-microscopic double folding model. Ife J Sci. 2023;25(2):239–50. Available from: https://www.ajol.info/index.php/ijs/article/view/254013
27. Abenga RC, Ibrahim YY, Adamu ID. Double folding potential and the deuteron-nucleus inelastic scattering in the optical model framework. Open Access Libr J. 2023;10:1–16. Available from: https://doi.org/10.4236/oalib.1109550
28. Farid ME Azab, Alsagheer L, Alharbi WR, Ibraheem AA. Analysis of deuteron elastic scattering in the framework of the double-folding optical potential model. Life Sci J [Internet]. 2014;11(5):208–16. Available from: https://www.researchgate.net/publication/287245041_Analysis_of_deuteron_elastic_scattering_in_the_framework_of_the_double_folding_optical_potential_model
29. Burq JP, Hadinger G, Kouloumdjian J, Meyer J. Asymétries produites par les deutons de 28 MeV polarisés vectoriellement dans les diffusions élastiques 12C(d,d)12C, 28Si(d,d)28Si et 40Ca(d,d)40Ca. Nucl Phys A. 1970;149:488–500. Available from: https://doi.org/10.1016/0375-9474(70)91042-0
30. Betker AC, Gagliardi CA, Semon DR, Tribble RE, Xu HM, Zaruba AF. Deuteron elastic scattering at 110 and 120 MeV. Phys Rev C. 1993;48(4):2085–8. Available from: https://journals.aps.org/prc/abstract/10.1103/PhysRevC.48.2085
31. Bäumer C, Bassini R, van den Berg AM, De Frenne D, Frekers D, Hagemann M, et al. Deuteron elastic and inelastic scattering from 12C, 24Mg, and 58Ni at 170 MeV. Phys Rev C - Nucl Phys. 2001;63(3):037601–4. Available from: https://journals.aps.org/prc/abstract/10.1103/PhysRevC.63.037601
32. An H, Cai C. Global deuteron optical model potential for the energy range up to 183 MeV. Phys Rev C - Nucl Phys. 2006;73(5):054605–9.
33. Ibraheem AA. Analysis of deuteron-nucleus scattering using the Sao Paulo potential. Brazilian J Phys [Internet]. 2016;46(6):746–53. Available from: http://dx.doi.org/10.1007/s13538-016-0453-0s